IV. Magnetic Domain Walls, Domains & Magnetization process

(1) Magnetic domain wall
(2) Magnetic domains
(3) Magnetization process

Types of magnetic energy density

Exchange energy f_{ex} : the energy cost of a change in the direction of magnetization, which tends to keep adjacent magnetic moments parallel to each other

$f_{ex} = E_{ex}/a^3 = -(2JS^2/a^3)\cos\Theta_{ij} = A(\partial\Theta/\partial x)^2$

since $E_{ex} = -2J\,\boldsymbol{S}_i \cdot \boldsymbol{S}_j \cos\Theta_{ij} = 1 - \Theta_{ij2}/2$ ...., and $\Theta_{ij} = a\partial\Theta/\partial x$

Magnetostatic energy f_{ms} : mainly from a discontinuity in the normal component of magnetization across an interface, and a form of anisotropy due to sample shape

$f_{ms} = -\mu_o \boldsymbol{M}_s \cdot \boldsymbol{H}_d = (1/2)\mu_o N M_s^2 \cos^2\Theta$

Magnetocrystalline anisotropy energy f_a : the preference for the magnetization to be oriented along certain crystallographic directions.

Uniaxial materials : $f_a = K_{u1}\sin^2\Theta + K_{u2}\sin^4\Theta + \ldots$

Cubic materials : $f_a = K_1(a_1^2a_2^2 + a_2^2a_3^2 + a_3^2a_1^2) + K_2(a_1^2a_2^2a_3^2) + \ldots$

Magnetoelastic energy f_{me} : part of the magnetocrystalline anisotropy that is proportional to strain

Cubic materials : $f_{me} = B_1[e_{11}(a_1^2 - 1/3) + e_{22}(a_2^2 - 1/3) + e_{33}(a_3^2 - 1/3)]$

$+ B_2(a_1a_2e_{12} + a_2a_3e_{23} + a_3a_1e_{31}) + \ldots$

Isotropic materials : $f_{me} = B_1e_{11}\sin^2\Theta = \lambda_s^2 E\cos^2\Theta = (3/2)\lambda_s\sigma\cos^2\Theta$

Magnetic potential energy(or Zeeman energy) f_{Zeeman} : the potential energy of a magnetic moment in a field.

$f_{Zeeman} = -\boldsymbol{M} \cdot \boldsymbol{B}$ - Why are magnetic domains and domain walls formed?

To reduce the magnetic energy (especially, magnetostatic energy) of a finite, uniformly magnetized sample

(1) Magnetic Domain Walls

❑ 180° Domain Wall : Simple model

- For the case of uniaxial anisotropy, K_u

Exchange energy E_{ex} contribution

$\sigma_{ex} \approx NE_{ex}/a^2 = JS^2\pi^2/Na^2$ ($\because E_{ex} \approx JS^2\Theta_{ij}^2 \approx JS^2(\pi/N)^2$)

Anisotropy energy E_{an} contribution

$\sigma_{an} \approx K_u Na$

The total domain wall energy density for a wall thickness of $\delta = Na$

$\sigma_{dw} = \sigma_{ex} + \sigma_{an} \approx JS^2\pi^2/Na_2 + K_u Na$

(see Fig. 8.3 and Fig. 8.4 in O'Handley)

The equilibrium wall thickness when $\partial\sigma_{tot}/\partial\delta = 0$

$\delta_{dw} = N_o a = \pi(JS^2/aK_u)^{1/2} = \pi(A/K_u)^{1/2}$

δ_{eq} ~ 0.2μm for low-anisotropy systems like soft magnetic materials

δ_{eq} ~ 10 nm for high-anisotropy systems like permanent magnets

Then $\sigma_{dw} = 2\pi(JS^2/aK_u)^{1/2} = 2\pi(A/K_u)^{1/2}$

Typical values of σ_{dw} ~ 0.1 mJ/m^2 (0.1 erg/cm^2)

- Micromagnetics of domain walls

$\delta_{dw} = \pi(JS^2K_u/a)^{1/2} = \pi(A/K_u)^{1/2}$

$\sigma_{dw} = 4(JS^2K_u/a)^{1/2} = 4(A/K_u)^{1/2}$

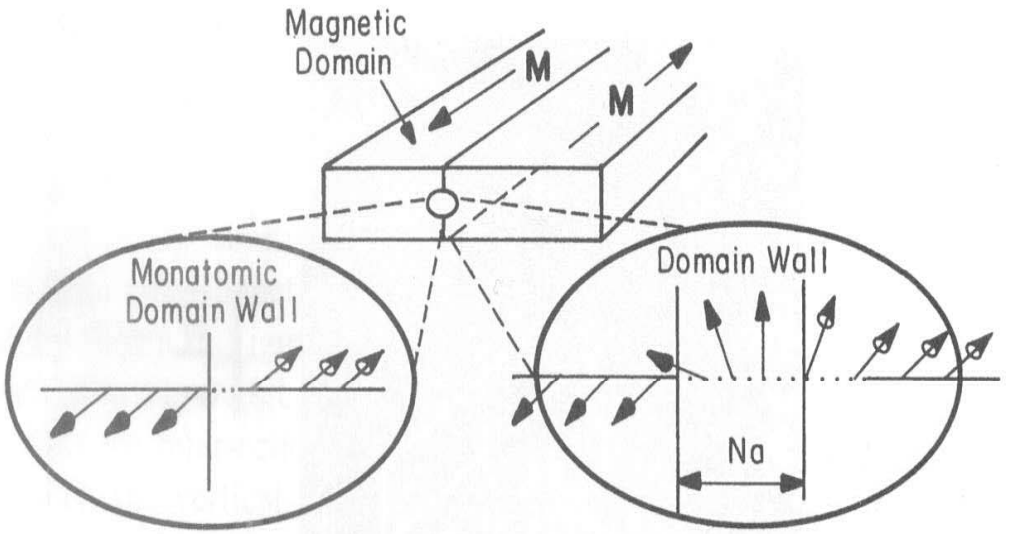

Figure 8.2 Schematic of ferromagnetic material containing a 180° domain wall (center). Left, hypothetical wall structure if spins reverse direction over one atomic distance. Right, wall structure if spins reverse direction over N atomic distances, a. In real materials, N is found to range from about 40 to nearly 10^4.

(1) Magnetic Domain Walls (continued)

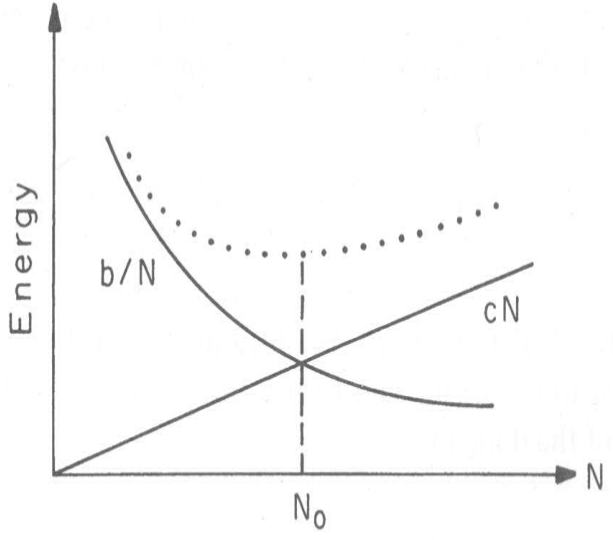

Figure 8.3 Minimization of the sum of exchange b/N and anisotropy cN energy densities occurs for $b/N = cN$, $N = \sqrt{(b/c)}$.

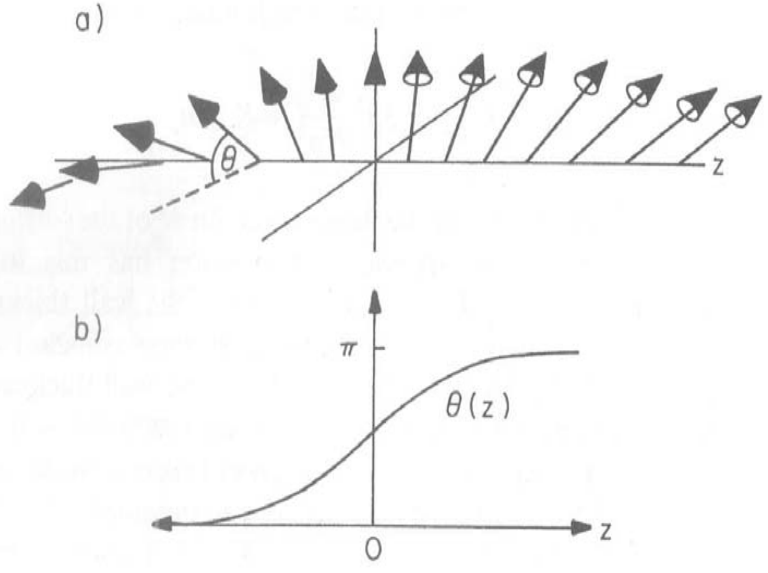

Figure 8.4 (*a*) Magnified sketch of the spin orientations within a 180° Bloch wall in a uniaxial material; (*b*) an approximation of the variation of θ with distance z through the wall.

(1) Magnetic Domain Walls (continued)

❑ Magnetostatic Effects on Domain Walls

For the wall structure near a surface or non-180° walls, the normal components of $\boldsymbol{M}$ is not continuous across a domain wall, a net pole density exists on the wall and associated magnetostatic field (or magnetostatic energy) results.

90° domain walls

90° walls : in materials of cubic anisotropy when the <100> directions are the easy axes like Fe

(cf. 180, 109, 71° walls : in materials of cubic anisotropy when the <111> directions are the easy axes like Ni)

- Two issues in defining the 90° domain wall.

(i) The continuity of the normal component of $\boldsymbol{M}$ across the wall

(ii) Rotation of magnetization within the wall in such a way to minimize the exchange and anisotropy energies

$\boldsymbol{M}_1 = \frac{M_s}{\sqrt{2}}(-1, -1, 0)$, $\boldsymbol{M}_2 = \frac{M_s}{\sqrt{2}}(-1, 1, 0)$, $\boldsymbol{n}_2 = (-\sin\psi, 0, \cos\psi)$

$(\boldsymbol{M}_1 - \boldsymbol{M}_2)\cdot\boldsymbol{n}_2 = 0$ for any $\psi \rightarrow$ uncharged 90° domain walls (see Fig. 8.6(a) in O'Handley)

In this case, the rotation path of magnetization (see Fig. 8.6(b) in O'Handley)

- Equilibrium wall thickness and wall energy density

$\delta_{dw}(90^o) = \delta_{dw}(180^o)/2$, $\sigma_{dw}(90^o) = \sigma_{dw}(180^o)/2$

- 180° walls in cubic materials (see Fig. 8.7 in O'Handley)

(1) Magnetic Domain Walls (continued)

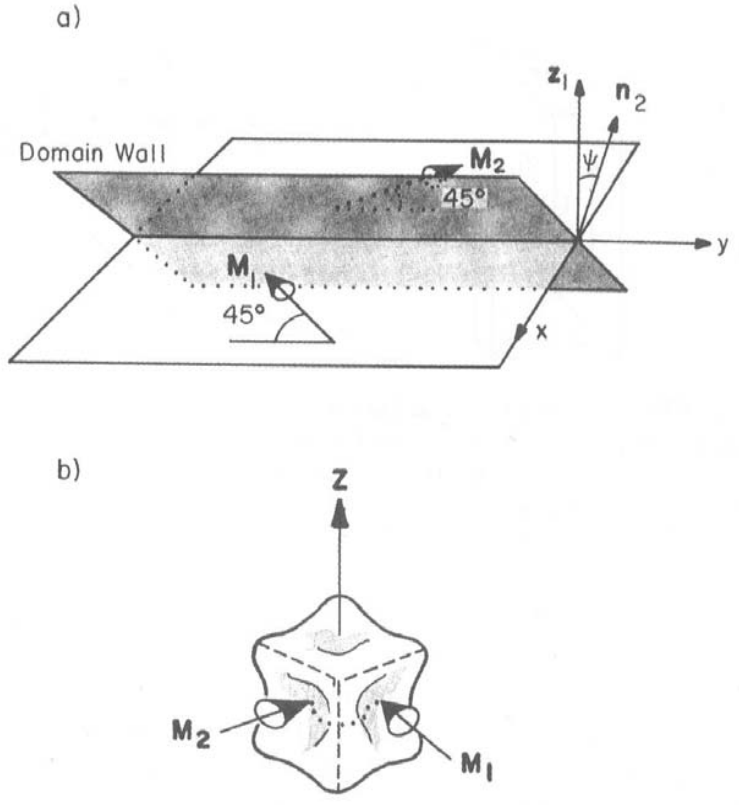

Figure 8.6 (*a*) The plane normal to *z* contains the domain magnetization vectors that are orthogonal to each other in cubic anisotropy [panel (*b*)]. The domain wall must lie in a plane that bisects the two directions of ***M***. A general plane satisfying this condition is shown shaded in (*a*); its normal direction, $\boldsymbol{n}_2$, must be chosen to minimize the wall energy. Panel (*b*) shows the cubic origin of the magnetization directions and the dotted line on the energy surface shows the minimal energy path between the two orientations.

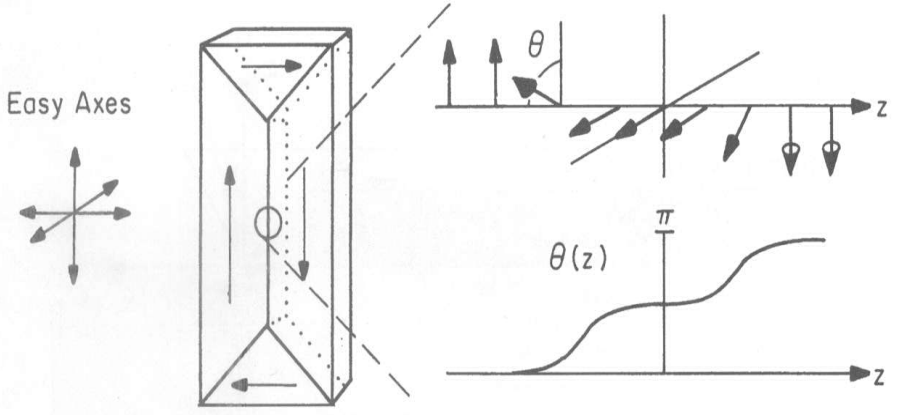

Figure 8.7 A (100) cut Fe single crystal has the possible domain pattern shown at left. The 90° walls are described in the text. The 180° wall may be thought of as a sequence of two 90° walls as shown at right. However, the inclusion of magnetoelastic energy stabilizes a 180° wall relative to the two 90° walls.

(1) Magnetic Domain Walls (continued)

Bloch vs Neel walls

-Difference between two walls
(see Fig. 8.8 in O'Handley)

Bloch walls : out-of-plane magnetization rotation

Neel walls : in-plane magnetization rotation

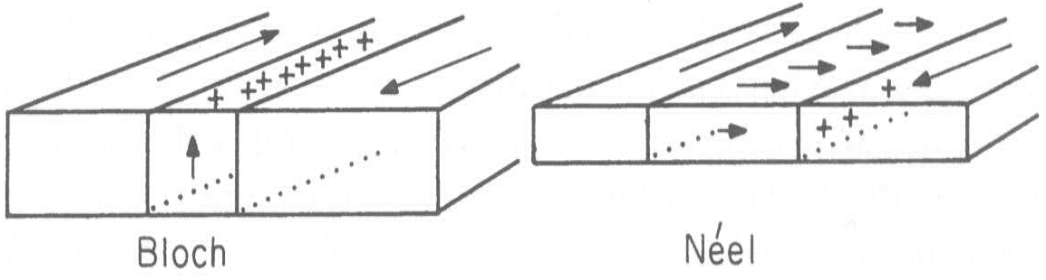

Figure 8.8 Comparison of Bloch wall, left, with charged surfaces on the external surfaces of the sample and Néel wall, right, with charged surfaces internal to the sample.

The magnetostatic energy of the domain wall in thin films can be minimized by forming Neel wall, and thus Neel walls are observed stable in various magnetic films for thickness up to ~ 60 nm.

(1) Magnetic Domain Walls (continued)

- Calculated film thickness dependence of the wall energy density and wall width, including magnetostatic energy terms for $t \approx \delta_{dw}$ (see Fig. 8.9 in O'Handley)

With decreasing film thickness, the Bloch wall energy density increases because of the increased magnetostatic energy due to the appearance of charged surface (or free poles), while the Neel wall energy decreases because it is proportional to the area of the charged surfaces inside the film.

To minimize the magnetostatic energy of the wall, while the Bloch wall width decreases with decreasing film thickness, the Neel wall width increases.
At sufficiently small film thickness, the magnetostatic energy is no longer significant and thus the Neel wall width is no longer increases.

- Thickness dependence of Neel walls :

$-\sigma_N \approx \pi t M_s^2$, $\delta_N \approx \pi(2A/K)^{1/2}$, $(t \ll \delta_N)$

where t is the film thickness

cf) $\delta_{dw} = \pi(A/K_u)^{1/2}$, $\sigma_{dw} = 4(A/K_u)^{1/2}$ for large-film-thickness forms of Bloch walls

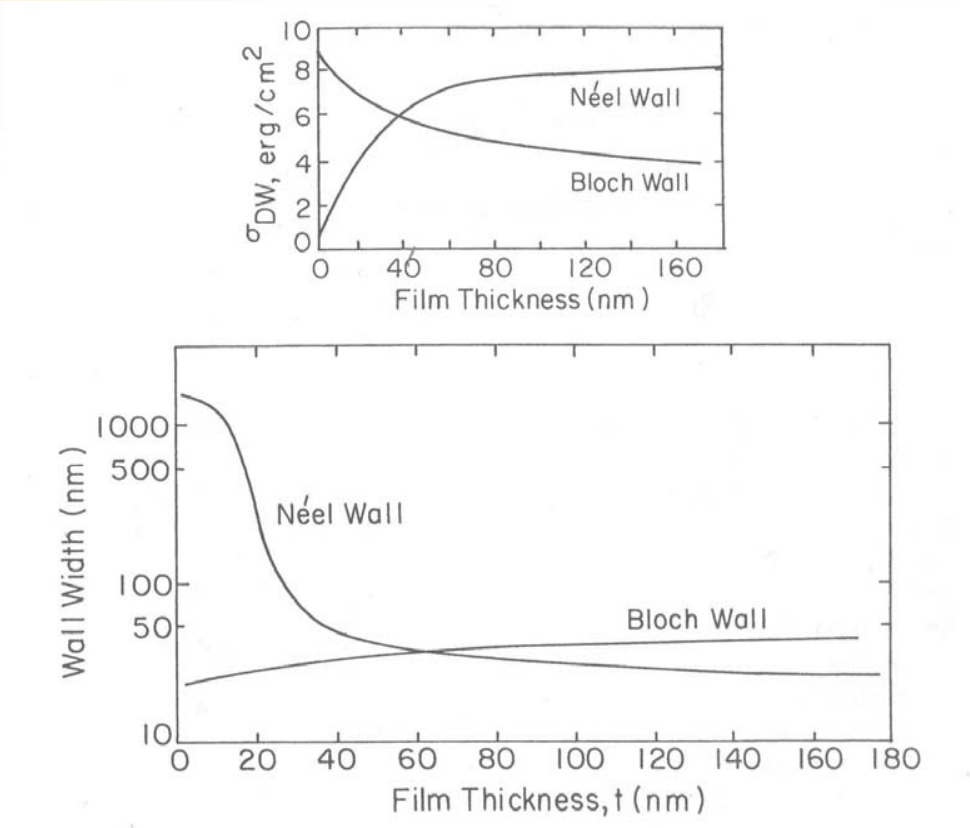

Figure 8.9 Energy per unit area (*a*) and thickness (*b*) of a Bloch wall and a Néel wall as functions of the film thickness. Parameters used are $A = 10^{-11}$ J/m, $B_s = 1$ T, and $K = 100$ J/m^3 [McGuire (unpublished)].

(1) Magnetic Domain Walls (continued)

- Recent experimental measurements and micromagnetic calculations of the surface magnetization distribution for $t > \delta_N$ (see Fig. 8.10 and 8.11 in O'Handley)

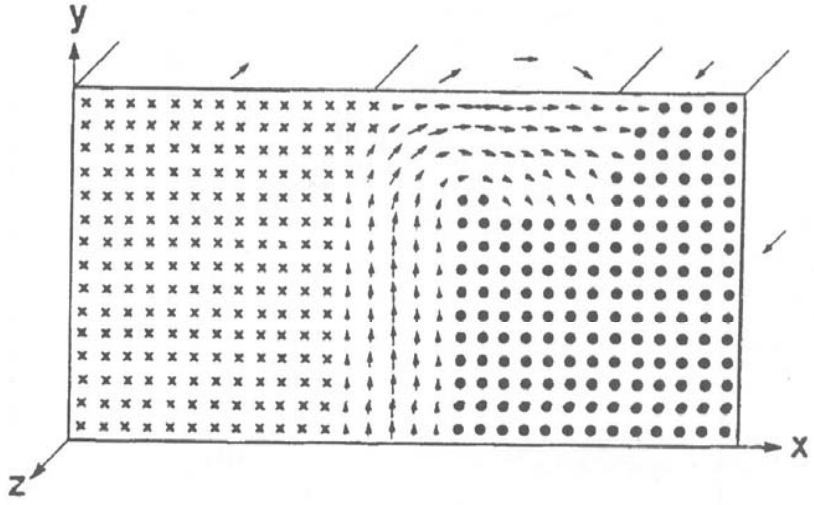

Figure 8.10 Calculated spin distribution in a thin sample containing a 180° domain wall. Note that the wall is a Bloch wall in the interior; specifically, M rotates 180° in the plane of the wall, but it is a Néel wall near the surface (to minimize magnetostatic energy), M rotates 180° passing through the wall normal (Scheinfein et al. 1989).

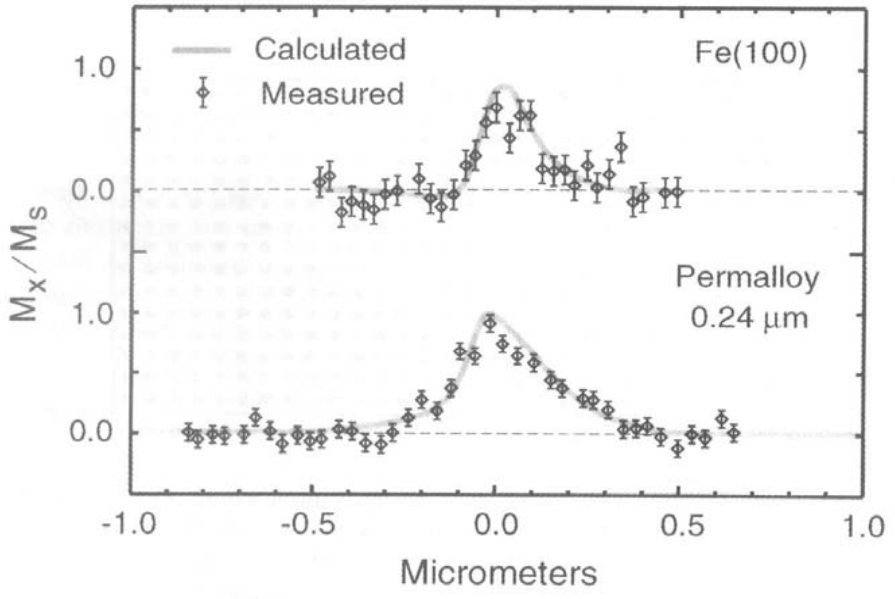

Figure 8.11 Measured (using SEMPA) and calculated surface wall profiles in a 20-μm-thick Fe whisker (top, $\delta_N \approx 0.2\,\mu$m) and a 0.24-$\mu$m-thick permalloy film (bottom, $\delta_N \approx 0.3\,\mu$m) (Scheinfein et al., 1991).

(1) Magnetic Domain Walls (continued)

Cross-Tie Walls

To minimize the magnetostatic energy by forming domains, a cross-tie wall is generated.

(see Fig. 8.12 and 8.13 in O'Handley)

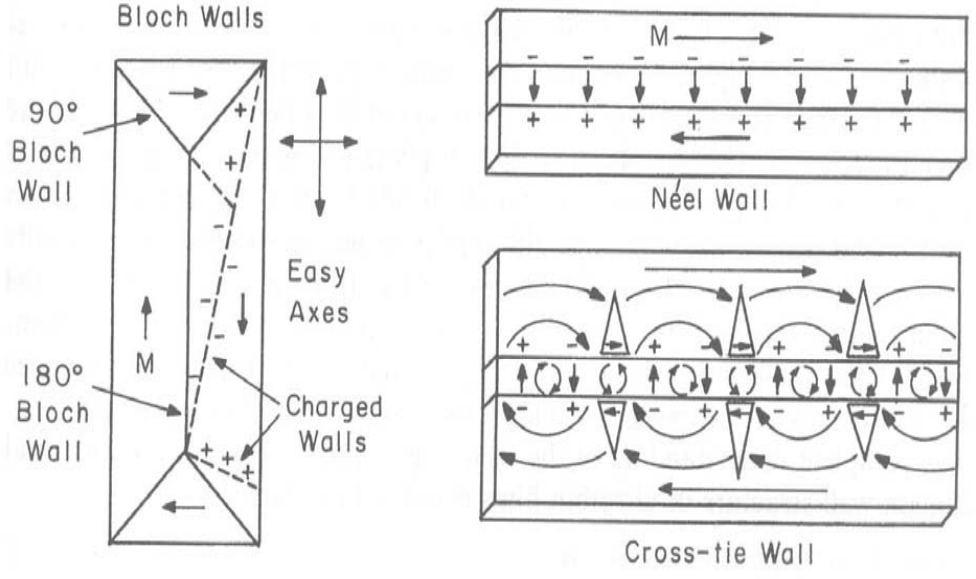

Figure 8.12 Left, Bloch wall showing how walls that do not follow the adjacent domain magnetization acquire a magnetic "charge"; Right, the charge on a Néel wall can destabilize it and cause it to degenerate into a more complex cross-tie wall.

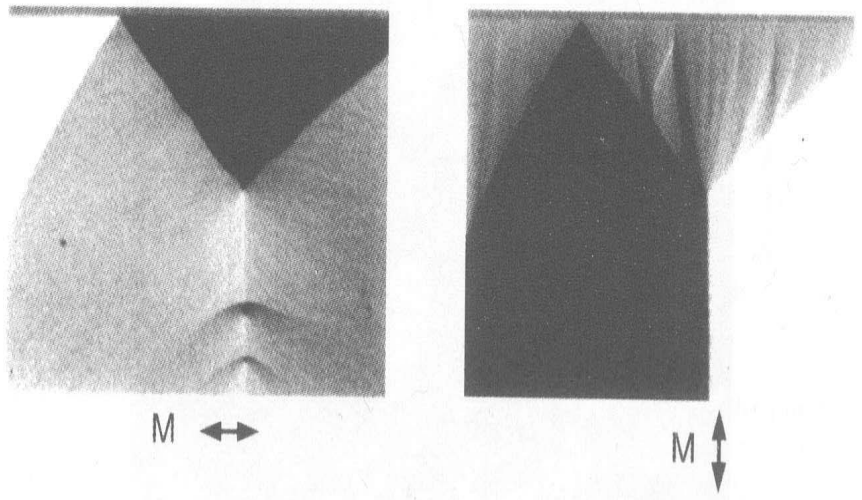

Figure 8.13 Scanning electron microscopy with spin polarization analysis (SEMPA) images of NiFe film. Panel (*a*) shows horizontal polarization contrast (white is magnetization to the right, dark to the left, and gray vertical). Panel (*b*) shows vertical polarization contrast near a triple-wall junction revealing cross ties on the domain walls. [Courtesy of Celotta et al. (1991).]

(1) Magnetic Domain Walls (continued)

Domain Walls in Ultrathin Films

The magnetization in the domains is perpendicular to the film plane and thus the magnetization inside 180° domain walls separating the domains lie in the film plane. However, the in-plane magnetization in the Bloch walls does not follow the <110> directions (i.e., easy axes) but domain walls tend to follow curved paths so as to minimize the wall energy. (see Fig. 8.14 in O'Handley for a Ni ultrathin film)

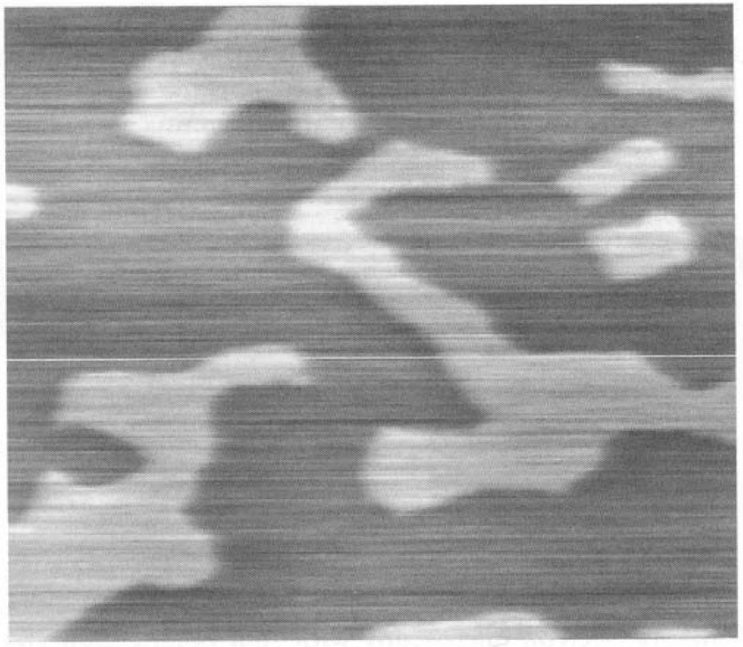

Figure 8.14 Magnetic force microscopy image (see Chapter 16) of the domains in a 20-Å-thick epitaxial Ni film in which the magnetization is perpendicular to the film plane. Field of view is 12.5 μm^2. [After Bochi et al. (1995).]

(1) Magnetic Domain Walls (continued)

Domain Walls near Interfaces: The Exchange Length

The exchange length l_{ex} (or pinned wall thickness) : the thickness of the magnetization orientation transition when the magnetization is pinned in a direction different from the easy axis in the interior of the material

(see Fig. 8.15 in O'Handley)

- Two cases

(i) No perpendicular magnetization component near the interface

M rotation is driven toward the easy axis

by the interior anisotropy energy.

$M_{//}$(parallel to interface) : $l_{ex}^{\parallel} = (A/K_u)^{1/2} = \delta_{dw}/\pi$

(ii) Non-zero perpendicular magnetization component near the interface ***M*** rotation is driven toward the easy axis by both the interior anisotropy energy and the magnetostatic energy associated with the charged interface.

$M_{\perp}$(perpendicular to interface) : $l_{ex}^{\parallel} = \{A/(K_u + 2\pi M_{\perp}^2)\}^{1/2}$

(see Table 8.1 in O'Handley)

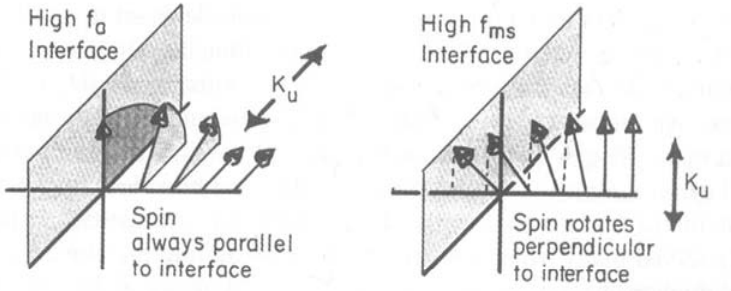

Figure 8.15 Illustration of the two cases important for determining the range of the twist in magnetization on moving from an interface at which the spins are pinned in a direction different from the interior of a ferromagnetic material. At left, the surface pinning holds the magnetization in the plane of the interface so magnetostatic energy is not an issue. At right, the surface spin pinning is such that a perpendicular component of magnetization exists near the interface. The magnetic charge at the interface gives rise to a local magnetostatic field that tends to shorten the exchange length.

(2) Magnetic Domain

Magnetic domain

Regions in a ferromagnetic material within which the direction of magnetization is largely uniform.

The orientation of *M* in each domain and the domain size:

determined by magnetostatic energy, crystal anisotropy energy, magnetoelastic energy, and domain wall energy

(exchange energy + anisotropy energy)

(see Fig 8.16 in O'Handley)

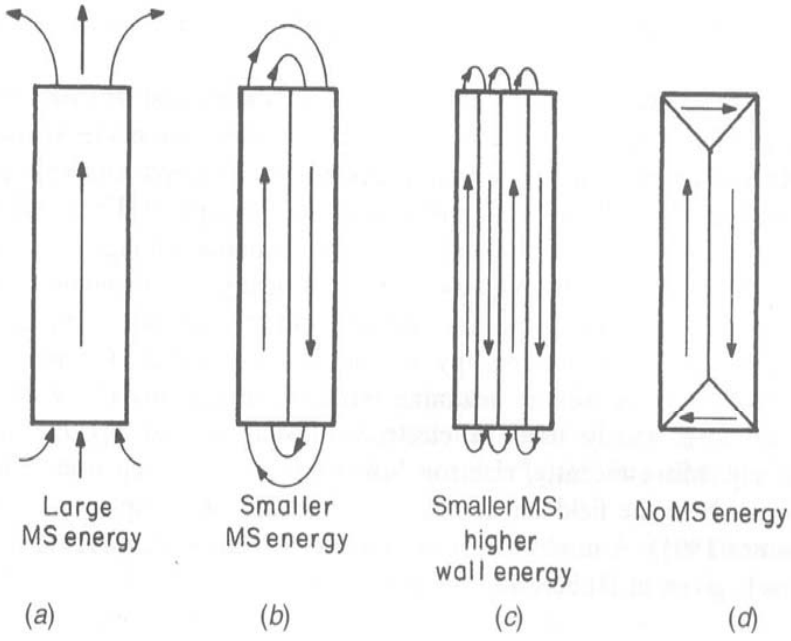

Figure 8.16 Domain formation in a saturated magnetic material is driven by the magnetostatic (MS) energy of the single domain state (left). Introduction of 180° domain walls reduces the MS energy but raises the wall energy; 90° closure domains eliminate MS energy but increase anisotropy energy in uniaxial materials and cause elastic energy due to the strain incompatibility of the adjacent 90° domains (right).

(2) Magnetic Domain (continued)

Magnetic materials with 180º walls:

Single domain is subdivided into multidomains to minimize the magnetostatic energy until the domain wall energy is greater than the magnetostatic energy saved.

Magnetic materials with cubic anisotropy or of not too strong uniaxial anisotropy:

Closure domains may be formed at its ends. Energy cost in terms of magnetic anisotropy energy for a uniaxial material and in terms of magneotelastic energy

Observations of magnetic domains

(ref. Hubert and Schaffer, Magnetic Domains, Springer-Verlag, Berlin, 1998)

Bitter solution technique

Transmission electron microscopy in the Lorentz mode

Magneto-optic Kerr effect microscopy

Scanning electron microscopy with spin polarization analysis (SEMPA)

Magnetic force microscopy (MFM)

Electron holography

(2) Magnetic Domain (continued)

❑ Uniaxial Domain Wall Spacing

Equilibrium wall spacing of domain size *d* in a uniaxial magnetic materials (see Fig. 8.17 in O'Handley)

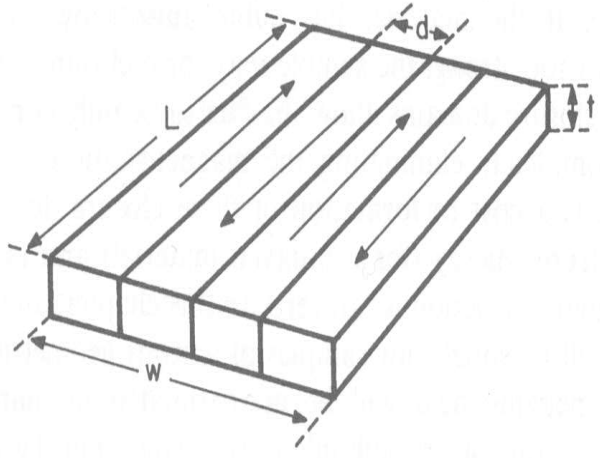

Figure 8.17 Geometry for estimation of equilibrium domain size in a thin slab of ferromagnetic material.

# of domains = W/d,

# of domain walls = W/d - 1

Area of a single wall = tL

Total domain wall energy, $F_w = \sigma_{dw}(W/d - 1)tL$

(2) Magnetic Domain (continued)

For a thin slab with the dimension of *W*(width) × *L*(length) × *t*(thickness)

Domain wall energy per unit volume,

$f_{dw} = F_w/LWt = \sigma_{dw}(W/d - 1)/W \approx \sigma_{dw}/d$

According to Kittel, the demagnetization factor N_d

$N_d/2 = 1.7d/L$ for the periodic array of domains for large t

$N_d/2 = (1.7d/L)(t/L)$ for small t

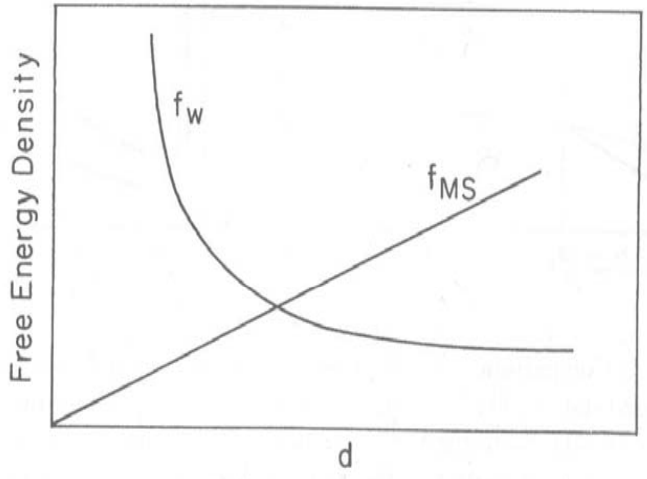

Figure 8.18 Variation of MS energy density and domain wall energy density with wall spacing *d*.

Magnetostatic energy density f_{ms} per unit volume

$f_{ms} = (N_d/2)\mu_o M_s^2$ (in SI unit) $= (1.7d/L)(t/L)\mu_o M_s^2$

Then, total energy density $f_{total} = f_{dw} + f_{ms} \approx \sigma_{dw}/d + 1.7(td/L^2)\mu_o M_s^2$

(see Fig. 8.18 in O'Handley)

(2) Magnetic Domain (continued)

Minimum energy when $\partial f/\partial d = 0$

→ equilibrium domain size(or wall spacing), d_o

$$d_o \approx L(\sigma_{dw}/1.7\mu_o M_s^2 t)^{1/2}$$

Then, the total energy density, $f_{total} = 2(1.7\sigma_{dw}\mu_o M_s^2 t)^{1/2}/L$

Interpretation: as t decreases, d_o increases and thus # of domains decreases because f_{ms} driving domain formation is reduced.

If t is smaller than a critical thickness t_c and thus f_{total} can exceed f_{mssd} of the single domain state,

$$f_{ms}^{sd} \approx \left(\frac{Wt}{L^2}\right)\left[\ln\left(\frac{4L}{W+t}\right) - 1\right]\mu_0 M_s^2$$

From $f_{total} = f_{mssd}$, $$t_c \approx 4\left(\frac{L}{W}\right)^2\left(\frac{1.7\sigma_{dw}}{\mu_0 M_s^2}\right)\left[\ln\left(\frac{4L}{W+t}\right) - 1\right]^{-2}$$

Interpretation: decreasing M_s, increasing L/W ratio, and/or increasing wall energy density σ_{dw} (higher K) would raise t_c. (see Fig. 8.19 in O'Handley)

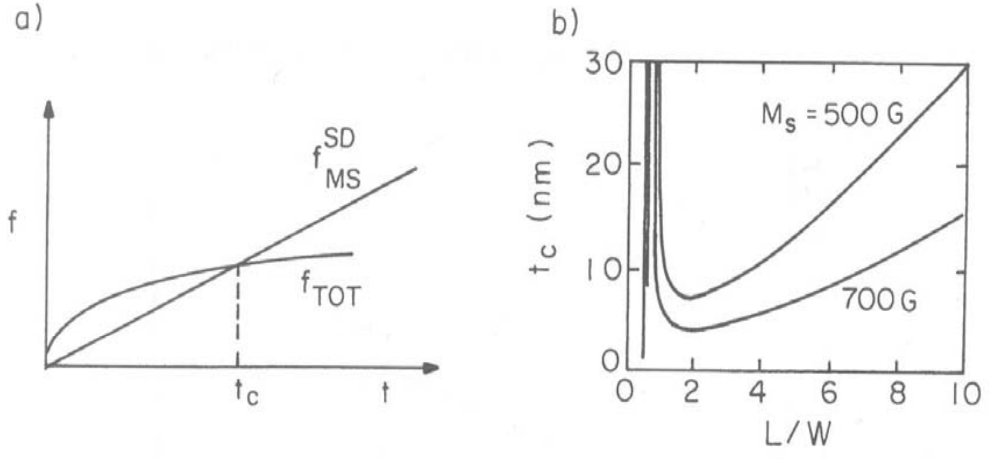

Figure 8.19 (*a*) Comparison of the thickness dependence of the free energy density for the demagnetized state f_{tot} [Eq. (8.23)] with the free energy density for the single domain state, f_{ms}^{sd} [Eq. (8.24)]. Note the crossover below which the energy is lower for the single-domain state. (*b*) Variation of the criticdal thickness with the ratio L/W for two different values of magnetization and $\sigma_{dw} = 0.1$ mJ/m^2.

(2) Magnetic Domain (continued)

❑ Closure Domains (see. Fig.8.20 in O'Handley)

Uniaxial anisotropy case

180° domain wall energy per unit volume, $f_{dw} \approx \sigma_{dw}/d$

Decrease in 180° domain wall length : a fraction of d/L

Increase in 90° wall length : a fraction of $2d/L$

Considering $\sigma_{90} = \sigma_{dw}/2$, increase in the wall energy

$= \sigma_{dw}(1 - d/L) + \sigma_{90}(2d/L) = \sigma_{dw}\{1 + (\sqrt{2} - 1)d/L\}$

$\rightarrow$ a factor of $(1 + 0.41d/L)$: $\triangle f_{dw} = 0.41\sigma_{dw}/L$

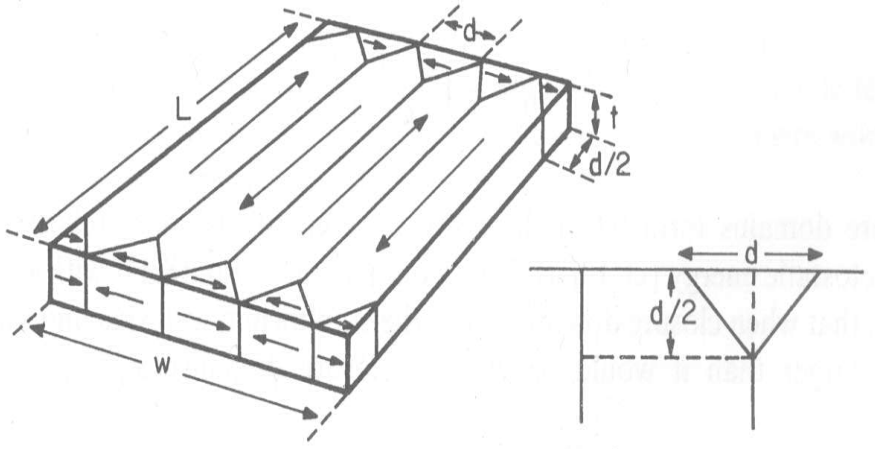

Figure 8.20 Geometry for estimation of equilibrium closure domain size in a thin slab of ferromagnetic material (cf. Fig. 8.18).

Since the magnetostatic energy reduces to zero, $\triangle f_{ms} \approx 1.7(td/L^2)\mu_o M_s^2$

On the other hand, since $2W/d$ closure domains are formed, increase in aniostropy energy of closure domains having each volume $d^2t/2$: $\triangle f_K \approx K_u d/L$

Thus, the energy change determining the closure domains is

$$\triangle f_{tot} \approx \triangle f_{dw} + \triangle f_K - \triangle f_{ms} = 0.41\sigma_{dw}/L + K_u d/L - 1.7(td/L^2)\mu_o M_s^2$$

(2) Magnetic Domain (continued)

$\triangle f_{tot} \approx \triangle f_{dw} + \triangle f_K - \triangle f_{ms} = 0.41\sigma_{dw}/L + K_u d/L - 1.7(td/L^2)\mu_o M_s^2$

Interpretation: (see Fig. 8.21 in O'Handley)

- If $\triangle f_{tot} < 0$, closure domains can be formed.

- Closure domains are favored in the cases of large M_s, large ratio of td/L^2, large t, small K_u, and small σ_{dw}.

- For L/d (or L/t) >>1, the spacing of the closure domains is represented by the spacing of the larger domains.

- For smaller aspect ratios, energy of closure domains ~ that of interior domain structure.

Then, $f_{tot} \approx (1 + 0.41d/L)\sigma_{dw}/d + K_u d/L$

Thus, the equilibrium wall spacing $d_o^{clos} \approx (\sigma_{dw} L/K_u)^{1/2}$

Since $d_o^{clos}/d_o = (\mu_o M_s^2 t/LK_u)^{1/2}$, $d_o^{clos} > d_o$

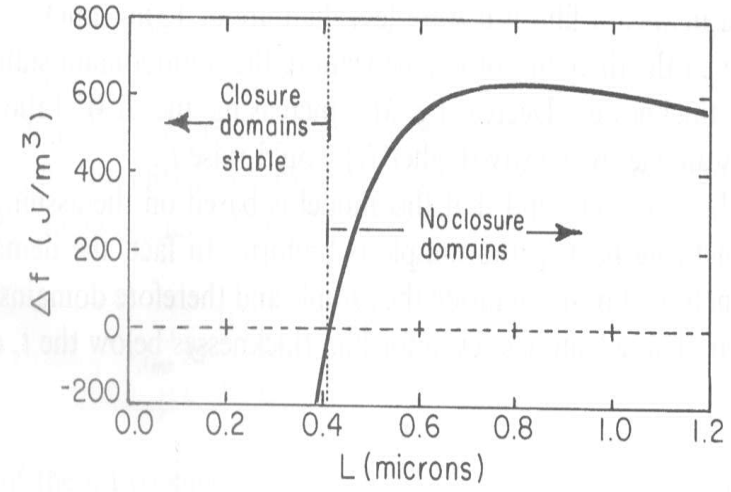

Figure 8.21 Energy density of Eq. (8.26) versus sample length L for $\mu_0 M = 0.625$ T, $\sigma = 0.1$ mJ/m^2, $K_u d = 1$ mJ/m^2, and $td = 10^{-14}$ m^2.

(2) Magnetic Domain (continued)

Cubic anisotropy case

Instead of anisotropy energy, magnetoelastic energy f_{me} is built up. Closure domain formation is still favored because of the dominance of the magnetostatic energy.

❑ Domains in Fine Particles

For a spherical particle with radius *r*,

Domain wall energy, $\sigma_{dw}\pi r^2 = 4\pi r^2 (AK_u)^{1/2}$

Magnetostatic energy saved by reducing the single domain state to multidomain sate, ignoring E_{ms} of the spherical particle composed of two equal domains,

$$\triangle E_{ms} \approx (1/3)\mu_o M_s^2 V = (4/9)\mu_o M_s^2 \pi r^3$$

Then, $r_c \approx 9(AK_u)^{1/2}/\mu_o M_s^2$; *acceptable approximation for large* K_u ($>> \mu_o M_s^2/6$)

For Fe, $r_c \approx 3$ nm, for ɣ-Fe_2O_3, $r_c \approx 30$ nm

(2) Magnetic Domain (continued)

If the anisotropy is not that strong,

three dimensional confinement of the magnetization twist increases the exchange energy contribution considerably. (see Fig. 8.22 in O'Handley)

The exchange energy density at the radius r

$$f_{ex}(r) = A(\partial\Theta/\partial x)^2) = A(2\pi/2\pi r)^2 = A/r^2$$

(see Fig. 8.23)

$$\langle f_{ex}\rangle = f_{ex}(r)drhd\phi = 4\pi A\int_0^R \frac{\sqrt{R^2 - r^2}}{r}dr$$

Here, $h = 2(R^2 - r^2)^{1/2}$.

Thus, $\langle f_{ex}\rangle = (3A/R^2)[\ln(2R/a) - 1]$

where, singularity at radius a (= lattice constant) of the symmetry

In this case, from $\triangle E_{ms} = \langle f_{ex}\rangle$,

$$r_c = (9A/\mu_o M_s^2)^{1/2}[\ln(2r_c/a) - 1]^{1/2} ;$$

acceptable approximation for small K_u

(see Fig. 8.24 in O'Handley)

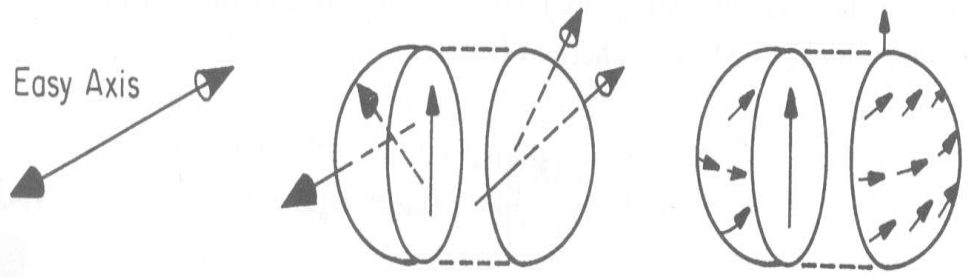

Figure 8.22 Left, model of a small ferromagnetic particle in which a domain wall similar to that in bulk material intersects the middle of the particle. Right, additional exchange energy is involved if the magnetization conforms to the surface of the particle.

(2) Magnetic Domain (continued)

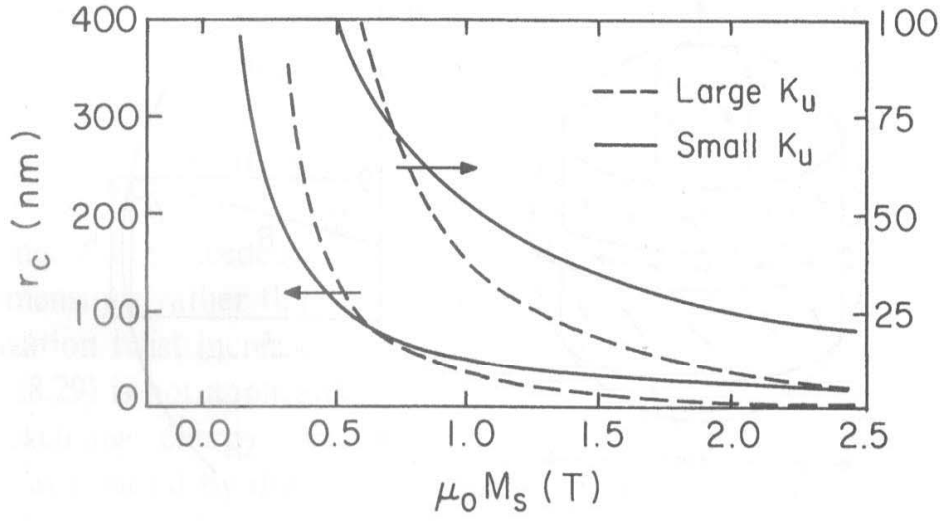

Figure 8.24 Critical radius for single-domain behavior versus saturation magnetization for spherical particles based on Eqs. (8.29) (large K_u, 10^6 J/m^3) and 8.31 (small K_u). Values of r_c for saturation magnetization greater than 0.5 Tesla are also shown magnified by a factor of 4 (right scale).

For an acicular iron particle of the same volume as a critical sphere, less energy is gained by introducing a domain wall because a larger aspect ratio reduces the magnetostatic energy and thus the critical volume for a single domain becomes larger than that of spherical particle.

(2) Magnetic Domain (continued)

For a platelike particle with in-plane anisotropy,

the critical volume becomes larger than that of spherical particle. However, for a platelike particle with out-of-plane anisotropy, E_{ms} is quite large and walls form more easily.

Superparamagnetism

Below a certain size, the remanent magnetization is no longer fixed in the direction dictated by particle shape or crystal anisotropy because of ambient thermal energy: a magnetic analog of Brownian motion. Typically below a radius of order 20 nm, magnetic particles become superparamagnetic.

▶ **Domains in Polycrystalline Materials**

The factor affecting the magnetization distribution and domain structure

- Magnetostatics- the system avoid charged surfaces and maintains

$(\boldsymbol{B}_1 - \boldsymbol{B}_2)\cdot\boldsymbol{n} = 0$

- $\boldsymbol{M}$ should follow the crystal and shape anisotropy easy axes subject to internal fields due to charged surfaces

- Exchange coupling will tend to maintain the direction of M across narrow, clean boundaries but not across wide, contaminated grain boundaries. (see Fig. 8.25 in O'Handley)

(2) Magnetic Domain (continued)

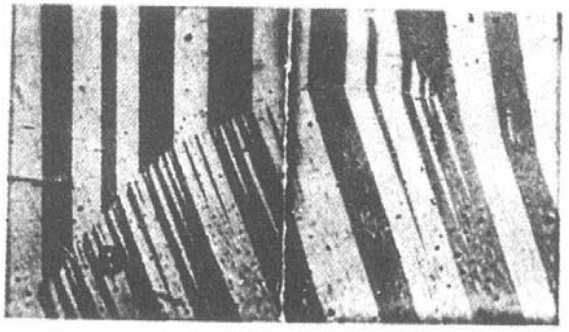

(a)

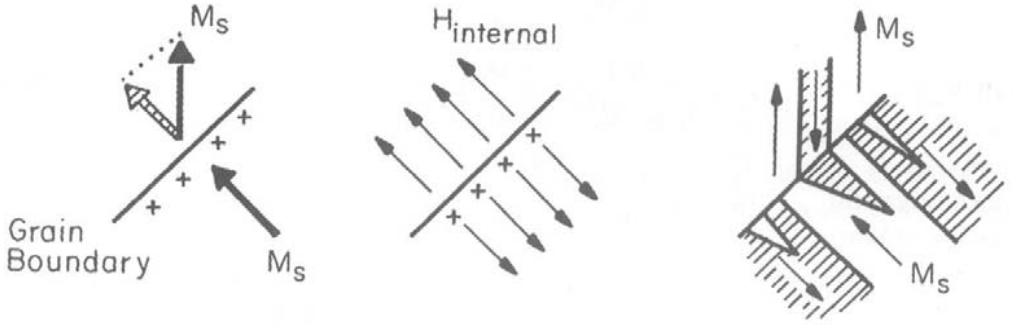

(b)

Figure 8.25 (*a*) Domains near a grain boundary in polycrystalline Fe–3%Si [after Shilling and Houze (1974)]; (*b*) process by which an imbalance in the normal component of magnetization across a boundary generates an internal field, which, in turn, favors the formation of reversal domains at the boundary.